

**ISC/25/ALBWG-01/08**

**Spatiotemporal modelling for size-specific CPUE standardization of albacore tuna  
in the north Pacific Ocean caught by Taiwanese longline fisheries**

Zi-Wei Yeh and Yi-Jay Chang

Institute of Oceanography, National Taiwan University, Taipei, Taiwan

[yjchang@ntu.edu.tw](mailto:yjchang@ntu.edu.tw)



## Abstract

This study applied size-specific spatiotemporal models to standardize catch-per-unit-effort (CPUE) of North Pacific albacore (*Thunnus alalunga*) from Taiwanese distant-water longline fisheries. Operational logbook records (1995 - 2024) and length-frequency samples (2004 - 2024) were integrated to construct daily size-specific CPUE, with albacore-targeted fleets identified through cluster analysis. Standardization was conducted using a delta-lognormal model in sdmTMB, incorporating spatial random effects and size-specific spatiotemporal variation. The resulting abundance indices revealed contrasting trends between life stages: adult abundance peaked in 2010 and 2013 but declined thereafter, whereas juvenile abundance increased sharply after 2018, reaching record highs in 2021 - 2022. These findings highlight the importance of size-specific modeling for developing robust abundance indices to support future stock assessments.

## 1. Introduction

Understanding spatial and temporal variations in size structure is critical for estimating the abundance of highly migratory fish, which often show size-based distribution patterns across their ranges (Kai *et al.*, 2017; Satoh *et al.*, 2021). In North Pacific albacore, smaller pseudo-cohorts are found at higher latitudes near Japan, while larger ones occur at lower latitudes in the western and central North Pacific (Ijima *et al.*, 2023). With the recent expansion of Taiwanese longline effort in the eastern Pacific Ocean (EPO), the ISC ALBWG recognized these data as a valuable source for developing juvenile abundance indices (ISC, 2024).

More recently, the ISC ALBWG (2025) recommended that the authors continue to refine a juvenile index, and—with lower priority—an adult index, from Taiwanese longline data. The Working Group also advised using smaller size bins rather than life-stage categories (Yeh *et al.*, 2024) when modeling size composition, so that standardized size compositions could be applied to estimate a selectivity curve for the juvenile index. Building on these recommendations, this study develops a size-specific spatiotemporal model to generate standardized size compositions for the Taiwanese longline fishery. The resulting indices will be submitted to the ISC ALBWG as candidate CPUE indices for use in future stock assessments.

## 2. Methods and materials

### 2.1 Data sources

This study utilized two data sources from the Taiwanese distant-water large-scale longline (DWLL) fishery, obtained by the Overseas Fisheries Development Council (OFDC), to estimate the relative abundance and size composition of albacore in the North Pacific Ocean (NPO).

#### (1) Fishery CPUE data from albacore-targeted fleets

Daily operational logbooks from Taiwanese longliners in the NPO from 1995 - 2024 were used in this study. The operational data included information on fish species, catch numbers, number of hooks, and location (longitude and latitude), with a resolution of  $1^\circ \times 1^\circ$  grid. CPUE is expressed as the number of fish caught per 1,000 hooks (N/1,000 hooks). This study employed a two-stage cluster analysis as described by He *et al.* (1997) to distinguish between albacore-targeted (ALB fleets) and non-albacore-targeted (non-ALB fleets) fleets within the Taiwanese DWLL fishery in the NPO during 1995 - 2024. Detailed methodology and procedures are presented in Hsu *et al.* (2022). The cluster analysis identified two distinct fleet types: fleets primarily targeting albacore tuna (ALB fleets) and fleets targeting bigeye and yellowfin tuna (non-ALB fleets) (**Figure 1**). The fishing characteristics of these fleets are presented in **Figure 2**, indicating that ALB fleets have higher albacore tuna catch, catch composition, and CPUE compared to non-ALB fleets. The spatial distribution of seasonal catch composition for both fleets is illustrated in **Figure 3**, showing that the ALB fleets primarily operate north of  $25^\circ\text{N}$ , with fishing activities concentrated in the first and fourth quarters. Based on these findings, this study uses only the CPUE data from the ALB fleets operating north of  $25^\circ\text{N}$  during the first and fourth quarters for standardization analysis. The spatiotemporal distribution of nominal CPUEs recorded by albacore-targeting fleets between 1995 and 2024 is shown in **Figure 4**.

#### (2) Length dataset

The length dataset (measured in cm), provided by the Overseas Fisheries Development Council (OFDC), comprises records of fish measured from catches of Taiwanese distant-water longline (DWLL) fleets operating in the North Pacific Ocean

(NPO). Since 1995, regulatory provisions have permitted the measurement of up to 30 fish per day, irrespective of species. Each record contains the vessel identification code, fishing date (year–month–day), species, fork length (continuous value), body weight (continuous value), and remarks (e.g., the sequential order of the specimen measured on that day). For albacore tuna, records from the dataset were extracted and grouped into 5-cm length intervals (from < 70 to  $\geq$  115 cm) to derive percentage size compositions. In this study, daily  $1^\circ \times 1^\circ$  size-specific CPUE data were constructed by merging the daily operational logbooks with the percentage size compositions, using vessel ID and fishing date as matching keys. Specifically, size-specific CPUE was calculated by multiplying the daily CPUE value by the corresponding percentage size composition. Due to data quality considerations, only data from 2004 to 2024 are included in this study. **Figure 5** presents bubble plots of catch and CPUE by length category (<75 to  $\geq$ 115 cm) from 2005 to 2020. The catch composition results indicate a shift from being dominated by fish <95 cm in length during 2004 - 2009, to a more balanced distribution of both small and large fish (with 85 - 95 cm most abundant), and then returning to a predominance of fish <95 cm after 2020. CPUE remained consistently high for fish in the 80 - 95 cm range throughout the time series; however, the CPUE of larger fish peaked during 2010 - 2012 and declined substantially after 2015.

## 2.2 Spatiotemporal analysis

sdmTMB was used to estimate size-specific CPUEs across different years and locations. We used a delta-lognormal approach (encounter rate and positive catch components) in both models to account for zero CPUE in the size data.

Encounter rate component (binomial distribution):

$$p(s, t, l) = \beta_p(t, l) + \omega_p(s) + \varepsilon_p(s, l, t)$$

Positive catch rate component (log-normal distribution):

$$q(s, t, l) = \beta_q(t, l) + \omega_q(s) + \varepsilon_q(s, l, t)$$

where  $\beta(t, l)$  is the fixed effect for size class  $l$  in each year  $t$ ;  $\omega(s)$  is the shared spatial random effect for each knot  $s$  among size classes;  $\varepsilon(s, l, t)$  is the spatiotemporal random effect for each knot  $s$  and group  $l$  in year  $t$  (interaction term of spatiotemporal and size class). In *sdmTMB*, this model structure is implemented by specifying separate

spatiotemporal fields for each size class, which is achieved by creating a new variable that concatenates size class and year. For example, size-specific spatiotemporal variation can be incorporated by setting the time argument to time = “size\_year” (see Model 3: species-specific spatiotemporal fields, <https://pbs-assess.github.io/sdmTMB/articles/multispecies.html>).

### 2.3 Estimated size-specific relative abundance

The predicted CPUE of albacore for size group  $l$  at  $s$  knot in  $t$  year ( $d(s,t,l)$ ) was calculated as:

$$d(s,t,l) = p(s,t,l) \times q(s,t,l)$$

where  $p(s,t,l)$  is the estimated encounter probability and  $q(s,t,l)$  is the expected positive catch rate.

The size-specific abundance for albacore ( $B(l,t)$ ) was then obtained by applying area-weighting across knots:

$$B(l,t) = \sum_{s=1}^{n_s} A(s) \times d(s,t,l)$$

where  $A(s)$  is the surface area associated with knot  $s$ , and  $n_t$  is the total number of knots.

### 2.4 Estimation of juvenile and adult abundance indices

Juvenile and adult abundance in year  $t$ , denoted as  $B^J(t)$  and  $B^A(t)$ , respectively, were calculated as follows:

$$B^J(t) = \sum_{l=1}^n B(l,t) * (1 - \text{Mature}(l))$$

$$B^A(t) = \sum_{l=1}^n B(l,t) * \text{Mature}(l)$$

where  $\text{Mature}(l)$  is the probability of maturity for fish in size class  $l$ , and  $n$  is the total number of size classes considered. The size-at-maturity relationship is shown in **Figure 6**, with maturity proportions derived from the 2023 Stock Synthesis (SS) model report file, based on the beginning length in season 1.

### 3. Results

#### 3.1 Cluster Analysis

#### 3.2 Size-Specific Abundance Index

The predicted average density for 2004 - 2024 and the spatial knot configuration used in the sdmTMB package are shown in **Figure 7**. In this study, we tested different parameter values for constructing the spatial mesh, which had only minor effects on the resulting abundance indices (results not shown). **Figure 8** presents time-series plots (2004 - 2024) of relative abundance indices for different fish size classes, standardized to annual means (i.e., values scaled around 1). The aggregated index (all sizes combined) shows a relatively stable trend, except for pronounced increases in 2010 and 2013, indicating that pooling across size classes tends to smooth interannual variation. In contrast, the largest size classes (105 - 120 cm) exhibit higher variability, with sharp peaks during 2010 - 2015 (some reaching a relative value of 4), followed by a decline and subsequent stabilization at lower levels. These classes also display wider confidence intervals, reflecting greater uncertainty. Intermediate size classes (85 - 100 cm) show moderate peaks over 2010 - 2015, though with less pronounced variation than the largest sizes, and stabilize at lower levels after 2016. The smallest size classes (70 - 80 cm) show no major peaks, but exhibit short-term fluctuations and occasional wide confidence intervals.

#### 3.3 Standardization size composition

The standardized size compositions from 2004 - 2024 consistently exhibit a dominant mode at 80 - 90 cm FL (**Figure 9a**), with standardized (model) curves closely matching the nominal (observed) data. The heatmap further highlights the persistent dominance of fish in this size range, but also reveals temporal shifts toward smaller sizes in recent years (post-2020), when 75 - 80 cm fish became particularly abundant (**Figure**

**9b).** The smallest size class ( $\leq 70$  cm FL) was consistently present, though always at relatively low abundance compared to the dominant mode. Its contribution varied across years and occasionally formed a truncated shape, showing higher proportions than expected from the otherwise declining trend with decreasing length, suggesting the entry of new recruits (e.g., 2004, 2006, 2016, and 2024; **Figure 9a**). While never dominant, this group likely provides an important signal of annual recruitment strength, and the standardized model appears to capture its temporal variability effectively.

### 3.4 Estimation of juvenile and adult abundance indices

The spatial distribution of predicted juvenile density from 2004 to 2024 across the North Pacific is shown in **Figure 10**. The results indicate a core habitat band between  $30^{\circ}\text{N}$  and  $40^{\circ}\text{N}$  where density is consistently highest, but with considerable interannual variability in both intensity and location. The distribution expanded most notably in 2007, 2013, and after 2021, whereas it was relatively restricted in 2004, 2009, 2015, and 2017. As this study focuses on juveniles, the spatial distribution of predicted adult density is not presented here.

Relative abundance indices for juveniles and adults exhibited contrasting temporal patterns between 2004 and 2024 (**Figure 11**). Adult abundance was highly variable in the early period, with pronounced peaks in 2010 and 2013, but subsequently declined and stabilized at low levels after 2018. In contrast, juvenile abundance showed moderate fluctuations through 2015, followed by a notable increase after 2018, reaching its highest levels in 2021 - 2022 before declining again in recent years.

## References

Anderson, S. C., Ward, E. J., English, P. A., and Barnett, L. A. (2022). sdmTMB: an R package for fast, flexible, and user-friendly generalized linear mixed effects models with spatial and spatiotemporal random fields. *BioRxiv*, 2022-03.

He, X., Bigelow, K. A., and Boggs, C. H. (1997). Cluster analysis of longline sets and fishing strategies within the Hawaii-based fishery. *Fisheries Research*, 31(1-2), 147-158.

Hsu J., C.-H. Yi, C.-W. Chang and Chang Y.J. (2022). Catch, length composition, and standardized CPUE of the North Pacific albacore caught by the Taiwanese distant-water longline fisheries in North Pacific Ocean from 1995 - 2021. ISC/22/ALBWG-02/07.

Ijima, H., Minte-Vera, C., Chang, Y. J., Ochi, D., Tsuda, Y., and Jusup, M. (2023). Inferring the ecology of north-Pacific albacore tuna from catch-and-effort data. *Scientific Reports*, 13(1), 8742.

ISC. (2024). Plenary Report of the 24st meeting of the international scientific committee for tuna and tuna-like species in the North Pacific Ocean.

Kai, M., Thorson, J. T., Piner, K. R., and Maunder, M. N. (2017). Spatiotemporal variation in size-structured populations using fishery data: an application to shortfin mako (*Isurus oxyrinchus*) in the Pacific Ocean. *Canadian Journal of Fisheries and Aquatic Sciences*, 74(11), 1765-1780.

Kristensen, K., Nielsen, A., Berg, C. W., Skaug, H., and Bell, B. M. (2016). TMB: automatic differentiation and Laplace approximation. *Journal of statistical software*, 70, 1-21.

Liu, H. I., Chang, S. K., and Wu, R. F. (2015). Overviews on fishery development, data collection and processing system of Taiwanese distant-water longline fishery in the Pacific Ocean.

Maunder, M. N., Hamel, O. S., Lee, H. H., Piner, K. R., Cope, J. M., Punt, A. E., Ianelli, J. N., Castillo-Jordán, C., Kapur, M.K., and Methot, R. D. (2023). A review of estimation methods for natural mortality and their performance in the context of fishery stock assessment. *Fisheries Research*, 257, 106489.

Satoh, K., Xu, H., Minte-Vera, C. V., Maunder, M. N., and Kitakado, T. (2021). Size-specific spatiotemporal dynamics of bigeye tuna (*Thunnus obesus*) caught by the longline fishery in the eastern Pacific Ocean. *Fisheries Research*, 243, 106065.

Thorson, J. T., Scheuerell, M. D., Shelton, A. O., See, K. E., Skaug, H. J., and Kristensen, K. (2015). Spatial factor analysis: a new tool for estimating joint species distributions and correlations in species range. *Methods in Ecology and Evolution*, 6(6), 627-637.

Thorson, J.T., 2019. Guidance for decisions using the Vector Autoregressive SpatioTemporal (VAST) package in stock, ecosystem, habitat and climate assessments. *Fish. Res.*, 210, 143-161.

WCPFC SC19. (2023). Stock assessment of albacore tuna in the North Pacific Ocean in 2023. WCPFC-SC19-SA-WP-08.

WCPFC SC20. (2024). Background Analyses and Data Inputs for the 2024 South Pacific Albacore Tuna Stock Assessment. SC20-SA-IP-05.

WCPFC SC20. (2024). Background analyses for the 2024 stock assessment of southwestern Pacific striped marlin. WCPFC-SC20-SA-IP-06.

Yuan, T. L., Xu, H., Lu, B. J., and Chang, S. K. (2024). Comparison of linear and nonlinear modeling approaches to develop an abundance index based on voyage and market data for a data-limited fishery. *Frontiers in Marine Science*, 11, 1344181.

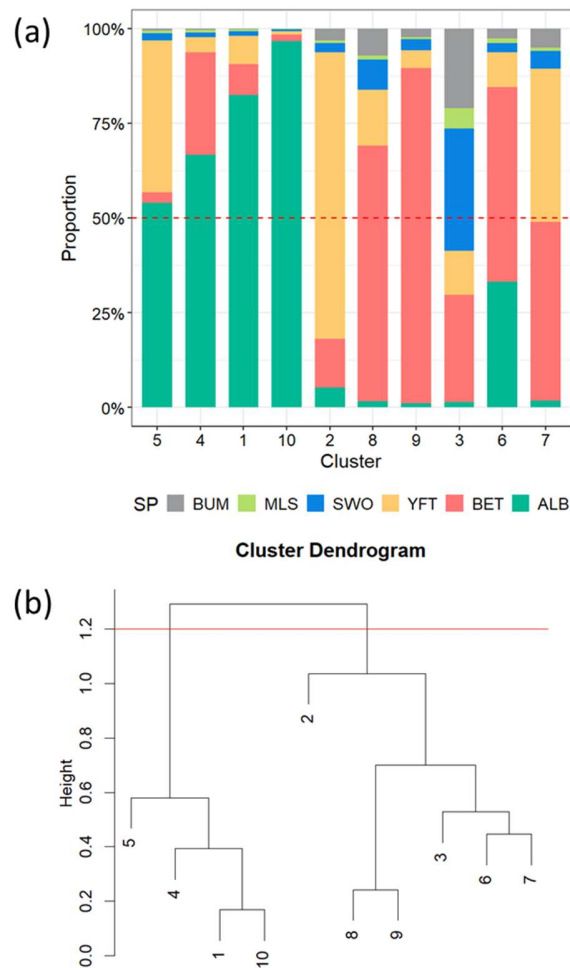


**Figure 1.** Cluster analysis of species composition from longline catches. (a) Proportional contribution of each species within clusters, where ALB = albacore, BET = bigeye tuna, YFT = yellowfin tuna, SWO = swordfish, MLS = striped marlin, BUM = blue marlin, and SP = other species. The dashed red line indicates the 50% threshold. (b) Dendrogram of hierarchical clustering showing relationships among clusters.

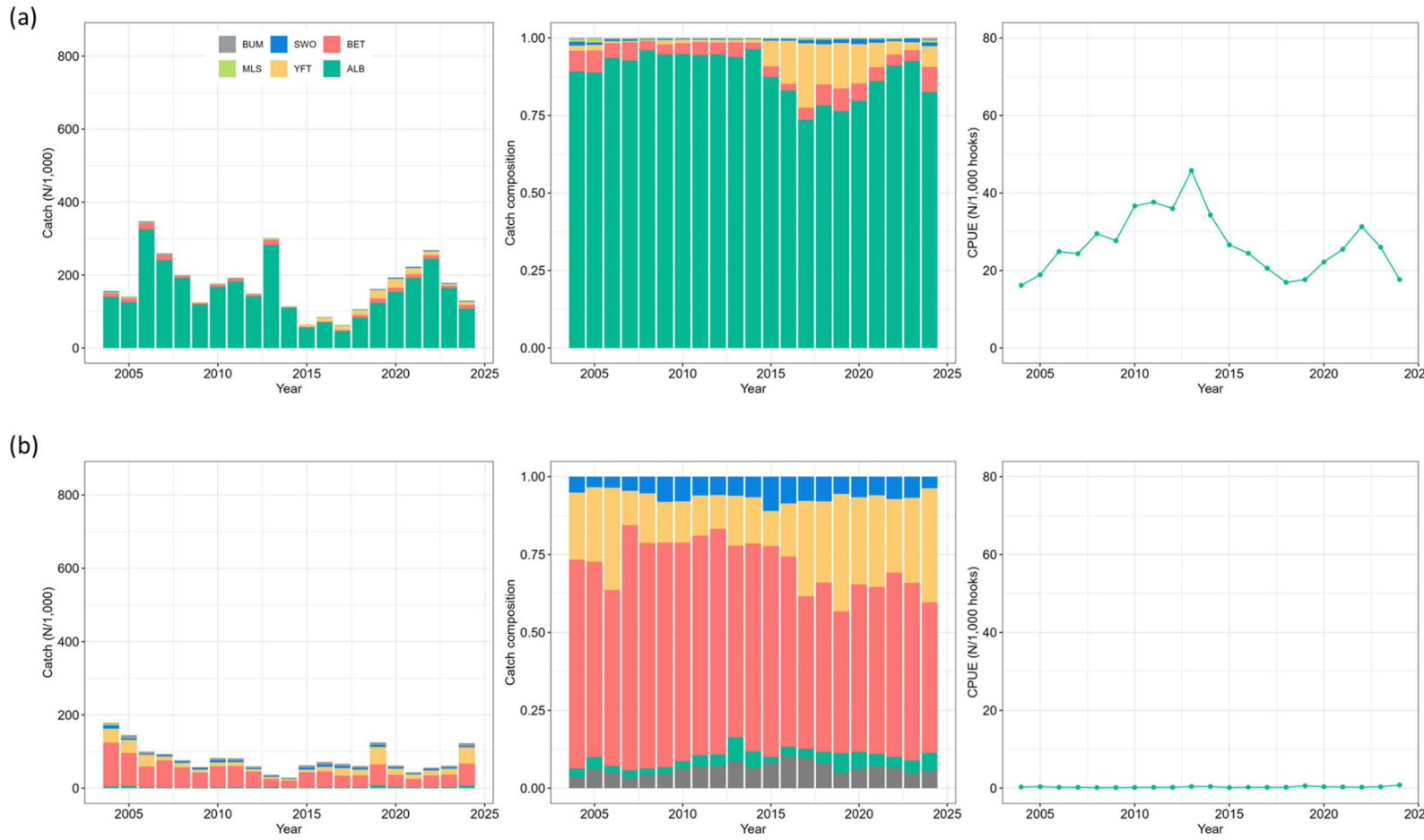


**Figure 2.** Catch (in numbers), catch composition, and albacore CPUEs (N/1,000 hooks) of the two clusters from 2004 to 2024: (a) the albacore-targeting fleet and (b) the non-albacore-targeting fleet.

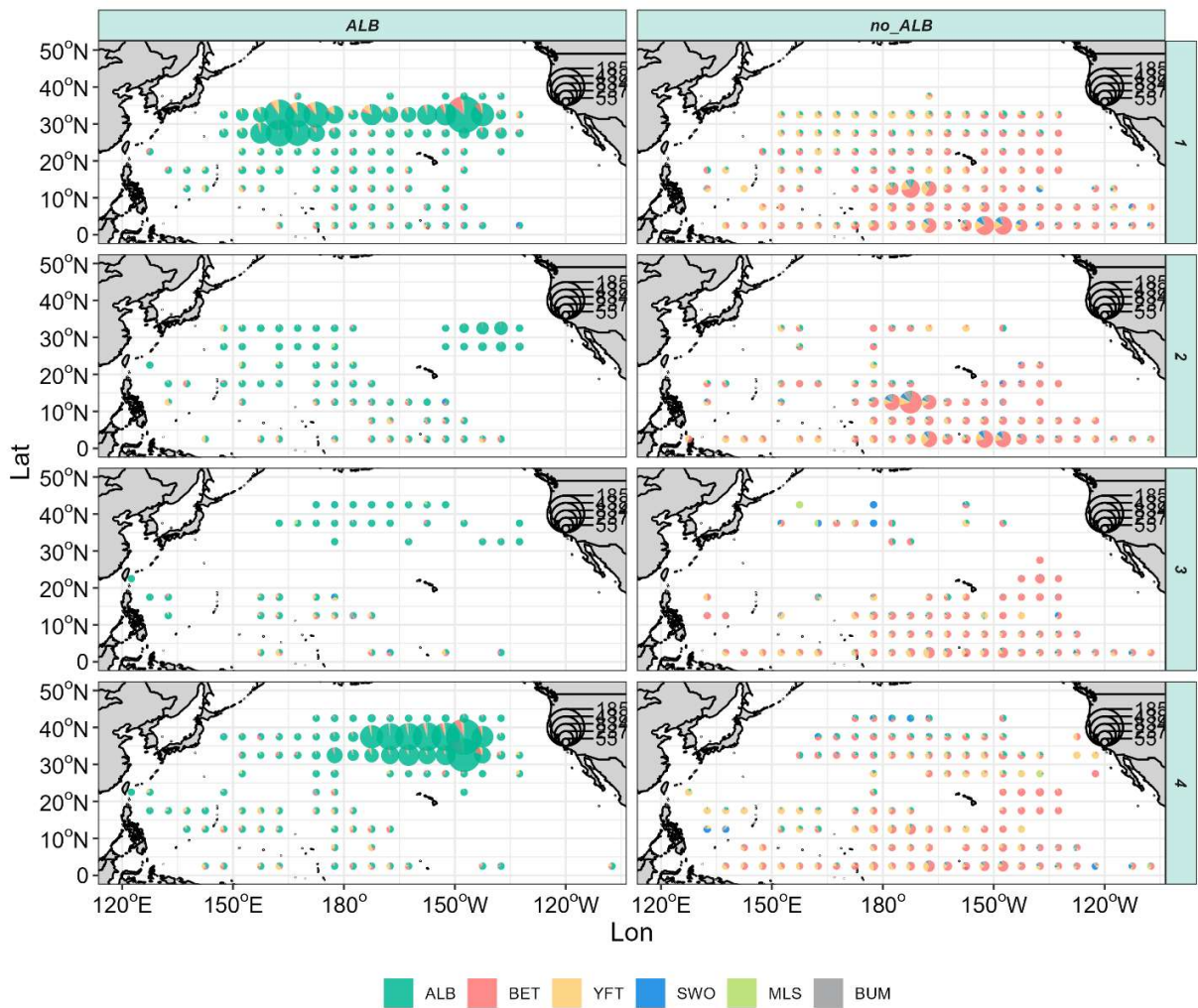


**Figure 3.** Spatiotemporal distribution of species composition in fish catches by different fleets (albacore-targeting vs. non-albacore-targeting) across seasons. Colors indicate species, and pie chart size is proportional to catch. Species codes: ALB = albacore, BET = bigeye tuna, YFT = yellowfin tuna, SWO = swordfish, MLS = striped marlin, BUM = blue marlin.

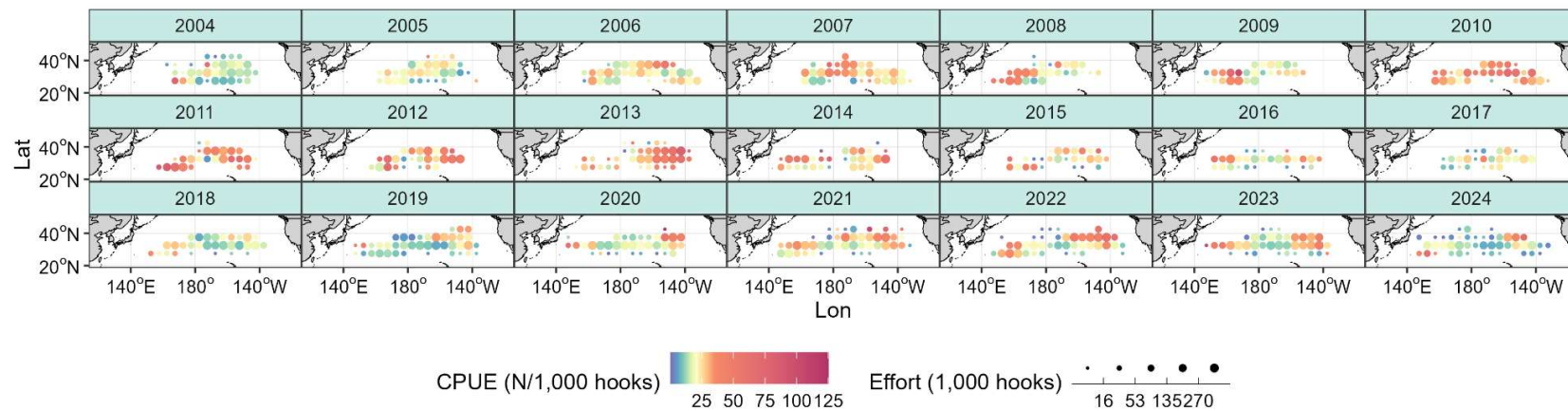


**Figure 4.** Spatial distribution of nominal catch-per-unit-effort (CPUE; number per 1,000 hooks) for albacore tuna by albacore-targeting fleets in the North Pacific Ocean, 2004 - 2024, with first and fourth quarters aggregated. CPUE is shown by color scale, and circle size represents fishing effort (1,000 hooks).

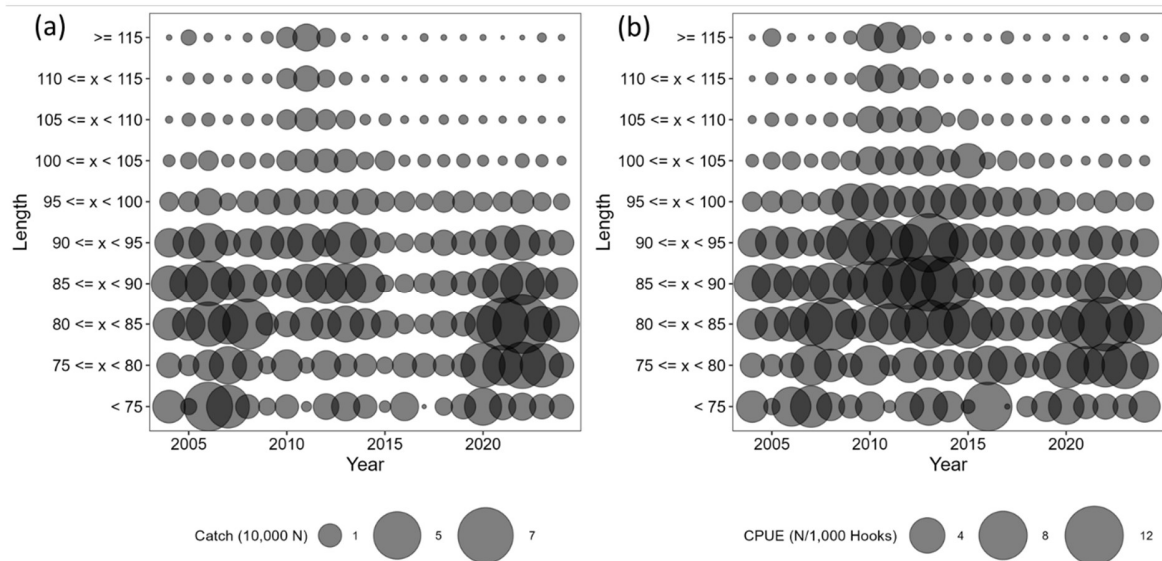


**Figure 5.** Bubble plots of (a) catch (in units of 10,000 fish) and (b) CPUE (number per 1,000 hooks) of albacore tuna by length class ( $<75$  to  $\geq 115$  cm) in the North Pacific Ocean from 2004 to 2024.

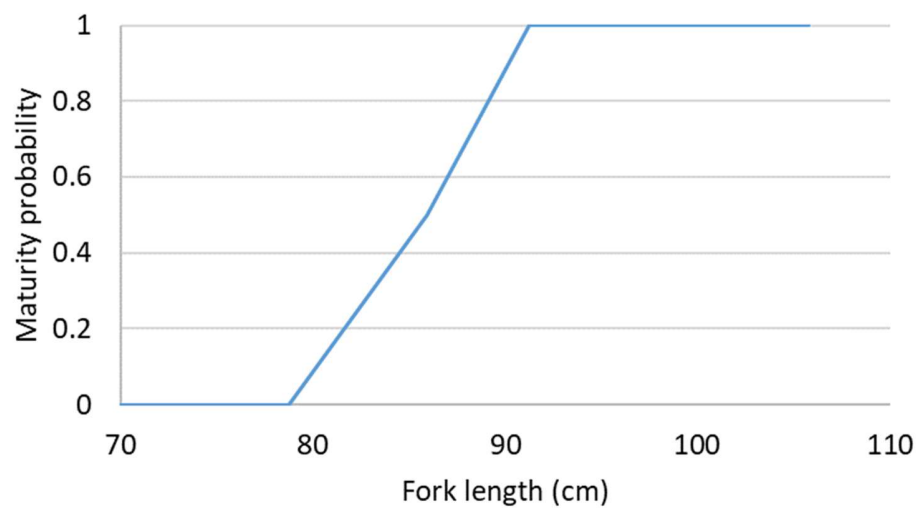


**Figure 6.** Maturity ogive of albacore tuna, showing the probability of maturity as a function of fork length.

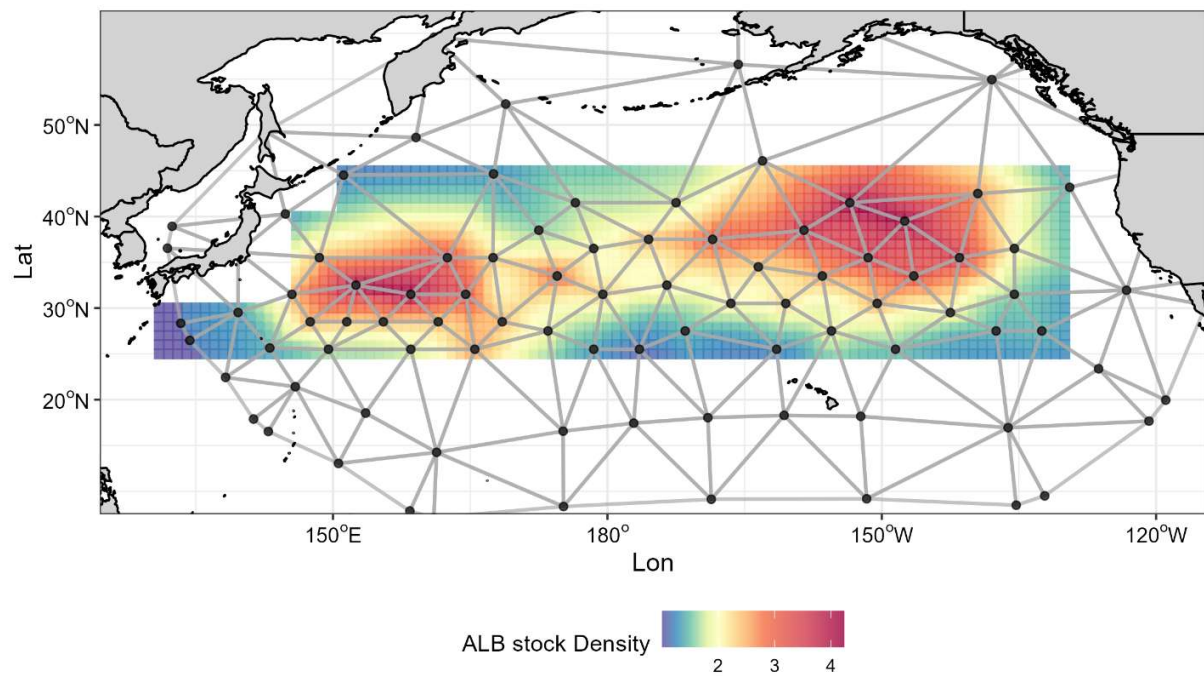


**Figure 7.** Spatial distribution of knots and estimated average albacore density (2004 - 2024) in the North Pacific Ocean from the sdmTMB model. Colored grids represent estimated density, and black dots indicate the spatial locations of knots used in the model.

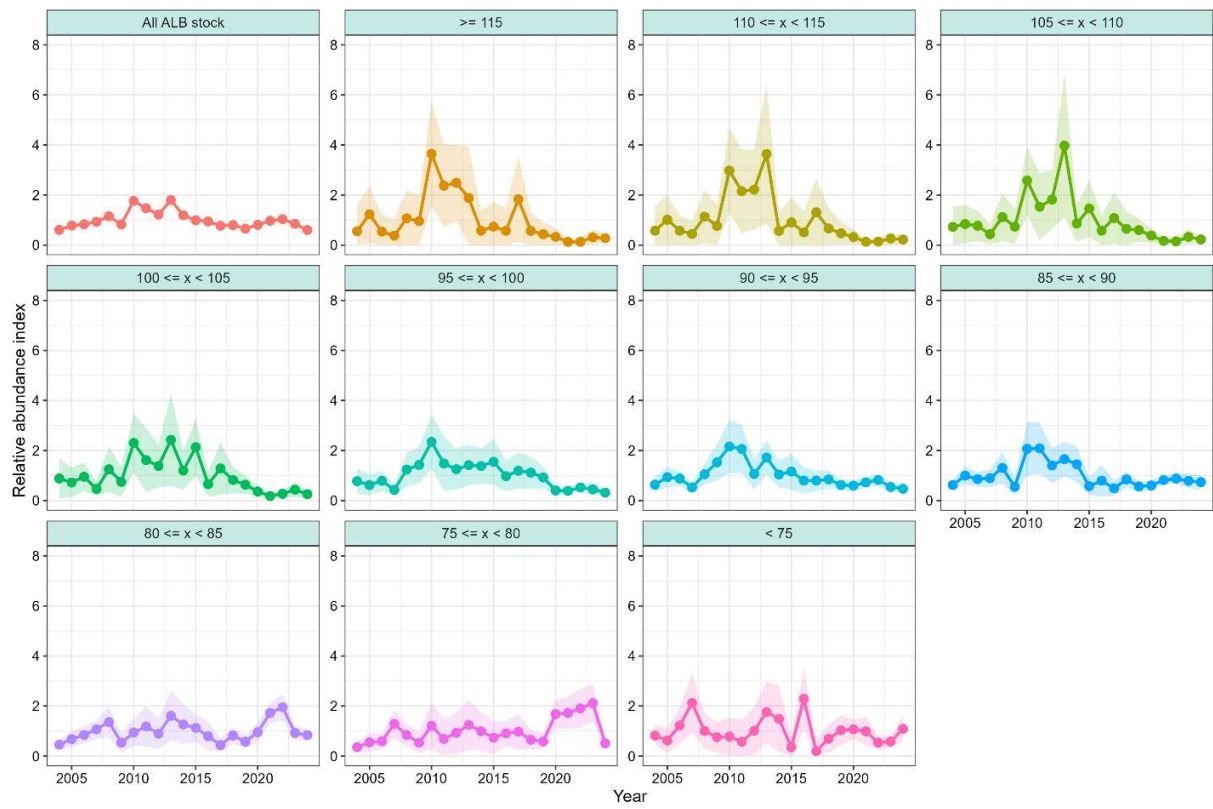


**Figure 8.** Standardized abundance indices of albacore tuna in the North Pacific Ocean from 2004 to 2024, shown for the entire size range (top left) and by 5-cm length classes ( $<75$  to  $\geq 115$  cm). Solid lines represent annual estimates, and shaded areas denote 95% confidence intervals.

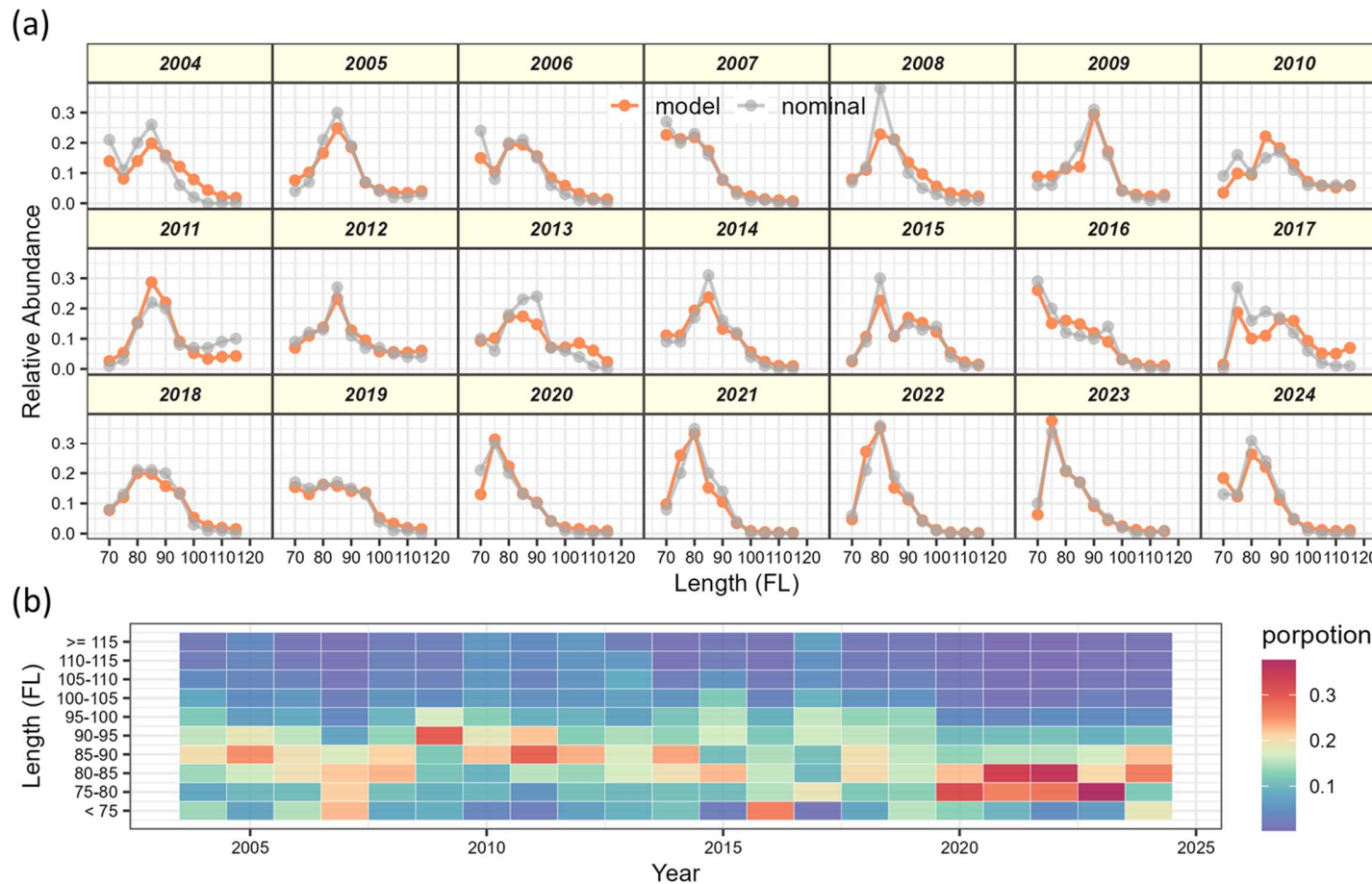


**Figure 9.** (a) Standardized length compositions of albacore tuna in the North Pacific Ocean from 2004 to 2024, showing model estimates (orange) compared with nominal observations (grey). (b) Heatmap of standardized length-frequency distributions, where colors indicate the proportion of fish in each 5-cm fork length class.

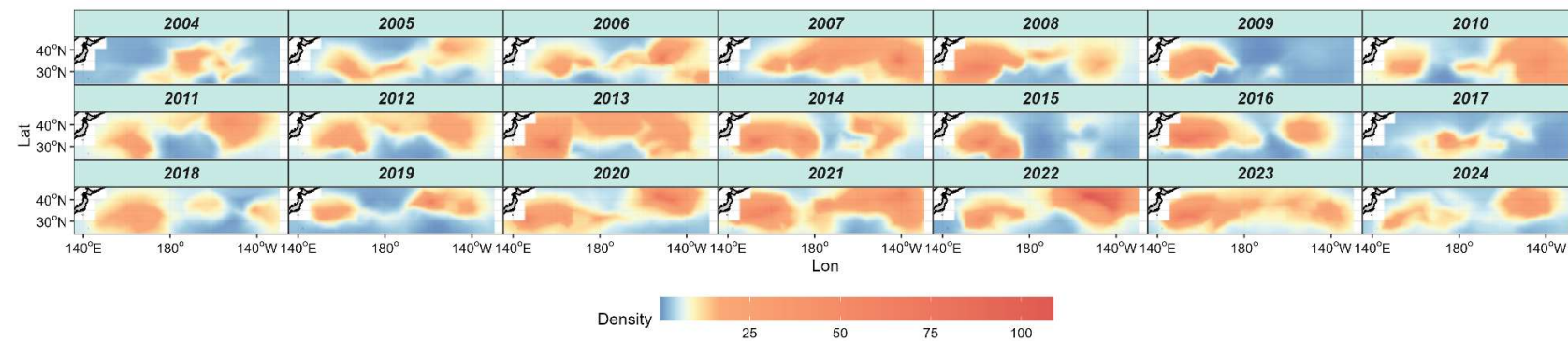


**Figure 10.** Annual spatial distribution of estimated juvenile albacore tuna density in the North Pacific Ocean, 2004 - 2024.

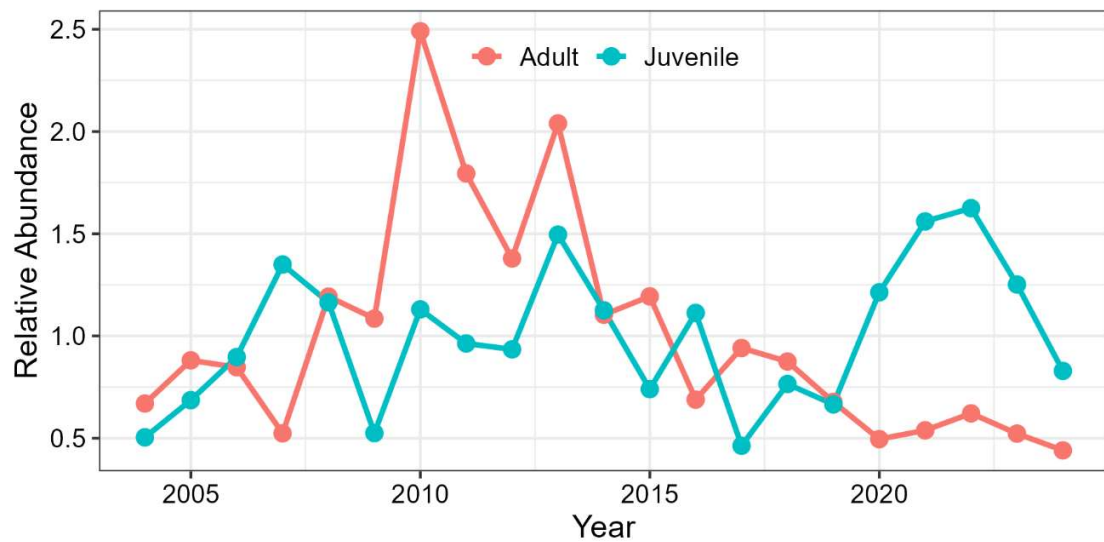


**Figure 11.** Time series of standardized relative abundance indices for adult and juvenile albacore tuna in the North Pacific Ocean, 2004 - 2024.